Developmental Biology 514 (2024) 109–116

Contents lists available at ScienceDirect

Developmental Biology

journal homepage: www.elsevier.com/locate/developmentalbiology

Tissue-specific and endogenous protein labeling with split fluorescent proteins

Gloria D. Ligunas [a,b,1], German F. Paniagua [a,1], Jesselynn LaBelle [a,b], Adela Ramos-Martinez [a], Kyle Shen [a], Emma H. Gerlt [a], Kaddy Aguilar [a], Ngoc Nguyen [a], Stefan C. Materna [a,b,c], Stephanie Woo [a,b,c,*]

[a] Department of Molecular and Cell Biology, University of California, Merced, CA, USA
[b] Quantitative and Systems Biology Graduate Group, University of California, Merced, CA, USA
[c] Health Sciences Research Institute, University of California, Merced, CA, USA

ARTICLE INFO

Keywords:
Zebrafish
CRISPR-Cas
Protein tagging
Split fluorescent protein

ABSTRACT

The ability to label proteins by fusion with genetically encoded fluorescent proteins is a powerful tool for understanding dynamic biological processes. However, current approaches for expressing fluorescent protein fusions possess drawbacks, especially at the whole organism level. Expression by transgenesis risks potential overexpression artifacts while fluorescent protein insertion at endogenous loci is technically difficult and, more importantly, does not allow for tissue-specific study of broadly expressed proteins. To overcome these limitations, we have adopted the split fluorescent protein system mNeonGreen2$_{1\text{-}10/11}$ (split-mNG2) to achieve tissue-specific and endogenous protein labeling in zebrafish. In our approach, mNG2$_{1\text{-}10}$ is expressed under a tissue-specific promoter using standard transgenesis while mNG2$_{11}$ is inserted into protein-coding genes of interest using CRISPR/Cas-directed gene editing. Each mNG2 fragment on its own is not fluorescent, but when co-expressed the fragments self-assemble into a fluorescent complex. Here, we report successful use of split-mNG2 to achieve differential labeling of the cytoskeleton genes *tubb4b* and *krt8* in various tissues. We also demonstrate that by anchoring the mNG2$_{1\text{-}10}$ component to specific cellular compartments, the split-mNG2 system can be used to manipulate protein localization. Our approach should be broadly useful for a wide range of applications.

1. Introduction

Protein labeling by fusion with genetically encoded fluorescent proteins has been a powerful tool for studying biological processes, allowing scientists to visualize and track proteins of interest in live cells. Fluorescent protein labeling has been especially useful for investigating the dynamic processes that occur during embryonic development. However, traditional methods for generating and expressing fluorescent fusion proteins, especially in multicellular organisms, have several drawbacks. In zebrafish and other model organisms, expression of fusion proteins can be achieved by injection of *in vitro* transcribed mRNA (Rosen et al., 2009), which is ubiquitous, or by transgenesis, which utilizes gene regulatory elements to drive spatiotemporal restricted expression (Clark et al., 2011). These approaches, however, run the risk of producing overexpression artifacts, in which proteins may not function or localize correctly when expressed at higher than wild-type levels (Simiczyjew et al., 2014). An alternative approach is to knock in fluorescent protein coding sequences into the genetic locus of that protein of interest (Albadri et al., 2017; Auer and Del Bene, 2014; Kimura et al., 2014). Although this approach has the advantage of preserving endogenous regulation of that protein's expression, many proteins are expressed broadly; issues arise when there is a need to study a broadly expressed protein in a specific tissue. Thus, there is a need for tissue-specific and endogenous tagging of proteins.

Split fluorescent proteins (split-FPs) are self-complementing protein fragments that only fluoresce when bound together. Split-FPs have been successfully used to visualize and quantify cell-cell interactions (Feinberg et al., 2008), signaling pathway activation (Harvey and Smith,

* Corresponding author. Department of Molecular anc Cell Biology, University of California Merced, 5200 N Lake Rd, Merced, CA, USA.
E-mail address: swoo6@ucmerced.edu (S. Woo).
[1] These authors contributed equally.

https://doi.org/10.1016/j.ydbio.2024.06.011
Received 3 March 2024; Received in revised form 18 June 2024; Accepted 19 June 2024
Available online 21 June 2024

2009), and subcellular protein localization (Cho et al., 2022). One commonly used split-FP system is based on the yellow-green fluorescent protein monomeric NeonGreen2 (mNG2) in which strands 1–10 of the mNG2 beta-barrel ($mNG2_{1-10}$) and strand 11 ($mNG2_{11}$) are expressed as independent protein fragments (Feng et al., 2017). On their own, the fragments are nonfluorescent, but when present in the same cell, they will self-assemble into a bimolecular complex with similar spectral properties to the intact, full-length fluorescent protein. The split-mNG2 system has been demonstrated to function in several different organisms and cell types (Cho et al., 2022; Kesavan et al., 2021; O'Hagan et al., 2021). Here, we adapt it for use in zebrafish to achieve tissue-specific and endogenous protein labeling. In our approach, $mNG2_{1-10}$ is expressed under the control of a tissue-specific promoter using standard zebrafish transgenesis techniques. Because the $mNG2_{11}$ fragment is only 16 amino acids long, its short sequence can be easily inserted into endogenous genetic loci by CRISPR/Cas-directed gene editing. In this way, the $mNG2_{11}$-tagged protein will continue to be expressed at endogenous levels, but fluorescent signal will only be detected in tissues in which $mNG2_{1-10}$ is co-expressed (Fig. 1A).

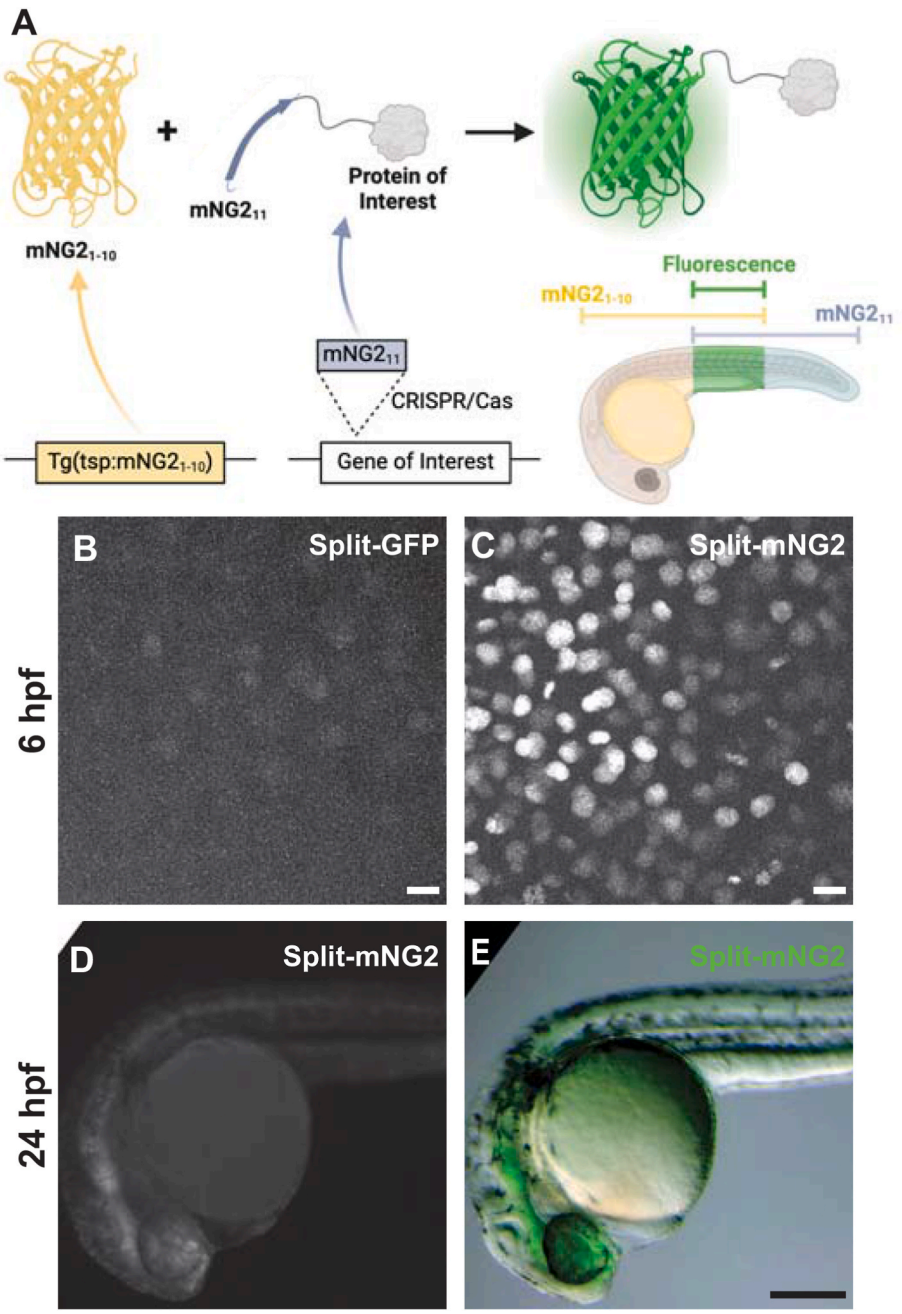

Fig. 1. Split fluorescent protein fragments are functional in zebrafish embryos. A. Schematic illustrating our protein labeling strategy using a split fluorescent protein. Transgenic (Tg) $mNG2_{1-10}$ is expressed under the control of a tissue-specific promoter (tsp) while $mNG2_{11}$ is inserted into protein-coding genes by CRISPR/Cas-directed gene editing. Fluorescence (green) is only generated in tissues co-expressing $mNG2_{1-10}$ and the $mNG2_{11}$-tagged protein of interest. **B–E.** Embryos were injected with GFP_{1-10} and GFP_{11}-H2B (split-GFP, B) or $mNG2_{1-10}$ and $mNG2_{11}$-H2B (split-mNG2, C–E) mRNAs then imaged at 6 h post-fertilization (hpf) on a confocal microscope (B, C) or at 24 hpf on a fluorescence stereomicroscope (D, E). Confocal images are displayed as maximum z-projections. Scale bars in B and C, 50 μm. Scale bar in E, 200 μm.

2. Results

2.1. $mNG2_{1-10}$ and $mNG2_{11}$ can assemble fluorescent complexes in zebrafish embryos

To assess the viability of our protein labeling strategy, we first determined if split-FP fragments could self-assemble in zebrafish embryos to form functional fluorescent complexes (Fig. 1B–D). We tested two different $FP_{1-10/11}$-type systems, split-GFP (Kamiyama et al., 2016) and split-mNG2 (Feng et al., 2017). We injected mRNAs encoding GFP_{1-10} and GFP_{11}-H2B (GFP_{11} fused to histone 2B) or $mNG2_{1-10}$ and $mNG2_{11}$-H2B ($mNG2_{11}$ fused to histone 2B) into zebrafish embryos. For both systems, expression of the FP_{1-10} or FP_{11} fragments alone did not produce fluorescence. However, when both fragments were co-expressed, we could detect nuclear-localized fluorescent signals by 6 h post-fertilization (hpf) using confocal fluorescence microscopy (Fig. 1B and C). We observed that embryos expressing split-mNG2 fragments (Fig. 1C) were brighter than those expressing the split-GFP fragments (Fig. 1B). Over time, split-mNG2 fluorescence remained brighter than split-GFP, which is consistent with a previous study showing that split-mNG2 can produce stronger fluorescence with less background compared to split-GFP (Feng et al., 2017). By 24 hpf split-mNG2 fluorescence was bright enough to be detected by a fluorescence stereomicroscope (Fig. 1D and E). Split-mNG2 fluorescence could still be detected after paraformaldehyde fixation even with some loss of brightness (Fig. S1). Based on these observations, we only used the split-mNG2 system for further experiments.

2.2. Generating $mNG2_{1-10}$ transgenic lines

We next determined whether transgene-driven expression of $mNG2_{1-10}$ could be used to spatially restrict fluorescence (Fig. 2). We generated multiple transgenic zebrafish lines that express $mNG2_{1-10}$ under control of various promoters representing a broad range of tissue types including *fezf2* (brain and eye) (Berberoglu et al., 2009), *myl7* (myocardium) (Huang et al., 2003), and *ubb* (ubiquitous expression) (Mosimann et al., 2011). To verify that these transgenic lines were functional, we injected transgenic embryos with $mNG2_{11}$-H2B mRNA, which would be distributed ubiquitously, and qualitatively assessed fluorescence patterns at 24 or 48 hpf. We found that uninjected $mNG2_{1-10}$ transgenic embryos exhibited no detectable fluorescence (Fig. S2). In contrast, transgenic embryos injected with $mNG2_{11}$-H2B mRNA exhibited fluorescence in spatially restricted patterns consistent with the promoter used to drive $mNG2_{1-10}$ expression (Fig. 2A–F). Compared to embryos expressing full-length, intact GFP under control of the same tissue-specific promoters, we found that GFP and split-mNG2 fluorescence were present in the same tissues and regions (Fig. 2G–L). In some cases, we observed minor differences in brightness that may be due to slight differences in staging or insertion-specific differences in transgene expression, but the overall pattern of tissue restriction was comparable between split-mNG2 and intact GFP lines.

2.3. $mNG2_{11}$ tagging by CRISPR/Cas-directed gene editing

We next determined whether proteins of interest could be tagged with $mNG2_{11}$ at their endogenous genetic loci by CRISPR/Cas-guided homology directed repair (Fig. 3). Previous reports have suggested that split-FP tagging works best for highly expressed genes (Goudeau

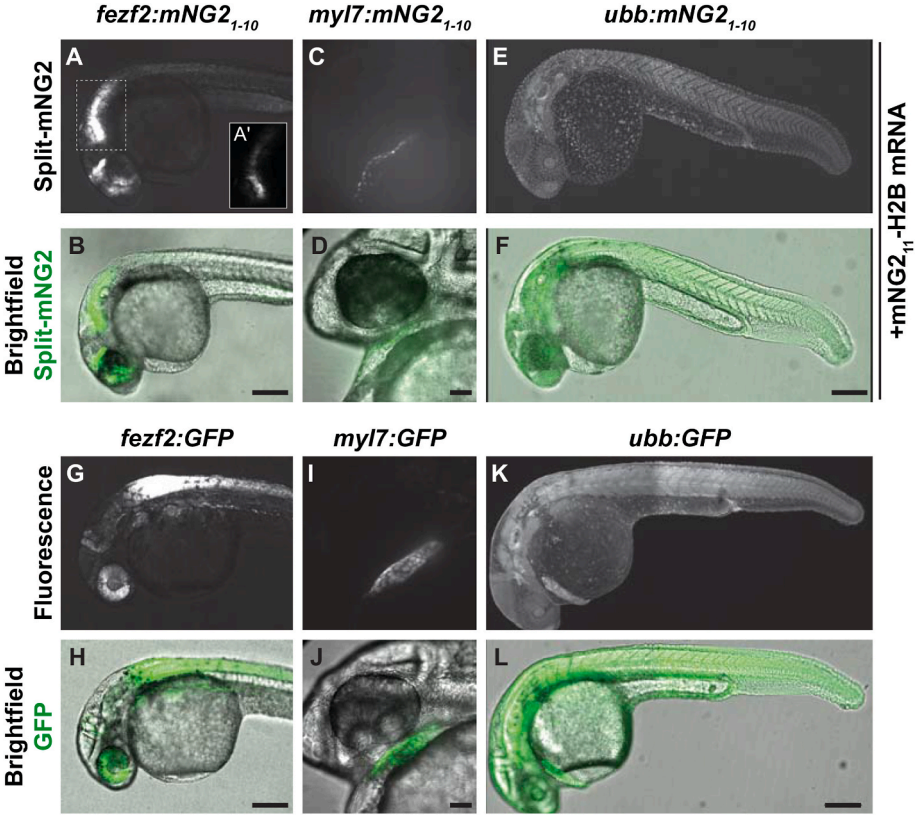

Fig. 2. Split fluorescent protein labeling can be spatially restricted by transgenic expression of $mNG2_{1-10}$. A–F. Transgenic embryos expressing $mNG2_{1-10}$ under control of the *fezf2* (A–B), *myl7* (C–D), or *ubb* (E–F) promoters and injected with $mNG2_{11}$-H2B mRNA. A′ shows the boxed region in A with brightness rescaled to demonstrate fluorescence is localized to nuclei. **G–L.** Transgenic embryos expressing GFP under control of the *fez1* (G–H), *myl7* (I–J), or *ubb* (K–L) promoters. Images were acquired at 24 h post-fertilization. Fluorescence images are maximum projections of confocal z-stacks. Scale bars in B, F, H, and L, 200 μm. Scale bars in D, J, 50 μm.

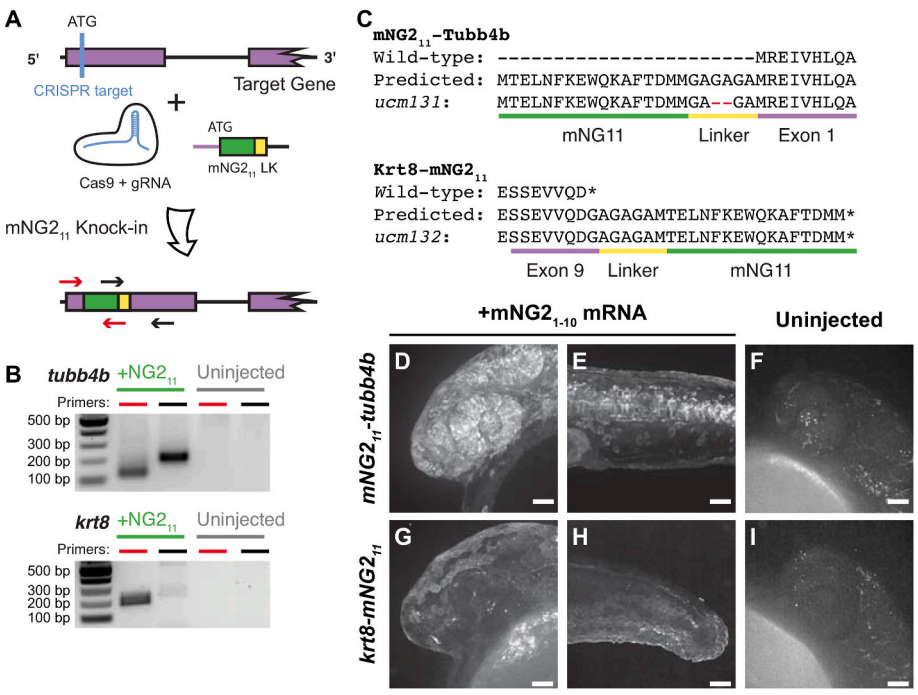

Fig. 3. mNG2$_{11}$ tagging by CRISPR/Cas-directed gene editing. A. Schematic of CRISPR/Cas-directed mNG2$_{11}$ insertion into target genes. Purple, endogenous exon sequence. Green, mNG2$_{11}$. Yellow, linker (LK). ATG, start codon. Arrows denote primers used in B. **B.** mNG2$_{11}$ insertion was assessed by PCR. The primers used correspond to the arrows shown in A. bp, base pairs. **C.** Amino acid sequences of wild-type, predicted mNG2$_{11}$ fusions, and recovered alleles for Tubb4b and Krt8. Mismatches between the predicted and recovered sequences are highlighted in red. Asterisks, stop codons. **D–I.** Representative images of *mNG2$_{11}$-tubb4b* (D–F) and *krt8-mNG2$_{11}$* (G–I) embryos injected with mNG2$_{1-10}$ mRNA (D–E, G–H) or uninjected (F, I). Maximum projections of confocal z-stacks. Images were acquired at 24 h post-fertilization. Images in F and I have been overexposed to emphasize lack of fluorescence. Scale bars, 50 μm.

et al., 2021; O'Hagan et al., 2021). Therefore, we targeted three genes that are highly expressed with relatively broad patterns — *tubb4b*, which codes for Beta-tubulin 4b; *krt8*, which codes for Keratin 8; and *h2az2b*, which codes for histone H2A. We designed guide RNAs (gRNAs) targeting each gene just downstream of the start (*tubb4b*) or upstream of the stop (*krt8, h2aza2b*) codon to generate, respectively, N- or C-terminal mNG2$_{11}$ tags. We injected gRNAs together with Cas9 mRNA and a repair template that contained the coding sequence for mNG2$_{11}$ and a short linker (Fig. 3A); the repair template consisted of double-stranded DNA with single-stranded homology arms of 30 bp at each end (Liang et al., 2017). To verify that the knock-in was successful, we pooled injected embryos and performed insert-specific PCR that amplified the mNG2$_{11}$ insertion but not the unedited wild-type (Fig. 3B).

For *tubb4b*, we estimated the knock-in efficiency using quantitative PCR. To determine mNG2$_{11}$ prevalence, we pooled and extracted DNA from 30 injected F$_0$ embryos at 24 hpf. We amplified mNG2$_{11}$ using insert-specific primers and amplified the untargeted, single-copy gene *prox1a* for comparison; we obtained a ΔCt of 5 cycles between the two. As zebrafish are diploid, *prox1a* is present in two copies per cell, but each mNG2$_{11}$ knock-in likely occurred only in one *tubb4b* allele per cell. We thus estimated that roughly 1 in every 16 cells in our pooled sample carried the knock-in allele, corresponding to a knock-in efficiency of about 6%, although not necessarily in-frame nor equally distributed among embryos. This knock-in efficiency is on par with other reports of CRISPR-guided knock-in in zebrafish (Auer and Del Bene, 2014; Zhang et al., 2023).

To establish stable, germline-transmitted lines for the mNG2$_{11}$ insertions, we raised injected F$_0$ fish to adulthood and identified several founders representing multiple alleles for each gene. Some alleles contained indel mutations at the insertion junctions or within the insertion itself. For example, both alleles recovered for *h2az2b* contained mutations within the mNG2$_{11}$ sequence and produced very dim fluorescence (Fig. S3). Therefore, we chose to propagate only alleles with precise integration of the mNG2$_{11}$ sequence, resulting in establishment of one line each for *tubb4b* (*tubb4b^{ucm131}*, referred to here as *mNG2$_{11}$-tubb4b*) and *krt8* (*krt8^{ucm132}*, referred to here as *krt8-mNG2$_{11}$*).

To confirm that the mNG2$_{11}$ tag is functional and does not alter endogenous expression patterns, we injected embryos with mNG2$_{1-10}$ mRNA and qualitatively assessed fluorescence. For *mNG2$_{11}$-tubb4b*, we observed strong fluorescence at 24 hpf that was especially prominent in the eye and brain (Fig. 3D) and along the neural tube (Fig. 3E). For *krt8-mNG2$_{11}$*, fluorescence appeared restricted to the skin epidermis at 24 hpf (Fig. 3G and H). These fluorescence patterns are consistent with the reported expression patterns for both *tubb4b* (Thisse and Thisse, 2008; Zhuo et al., 2012) and *krt8* (Fischer et al., 2014; Thisse and Thisse, 2008). At the subcellular level, we observed that fluorescence for both genes was enriched at the cell periphery and excluded from the nucleus, which would be expected for cytoskeletal filaments. For both genes, we observed no fluorescence in uninjected embryos (Fig. 3F–I)

2.4. Combinatorial expression of tissue-specific mNG2$_{1-10}$ and mNG2$_{11}$-tagged proteins

After successfully generating mNG2$_{1-10}$ transgenic lines and mNG2$_{11}$ insertions, we next determined whether these lines could be combined to achieve tissue-specific protein labeling (Fig. 4A). We crossed each of our mNG2$_{11}$-tagged lines — *mNG2$_{11}$-tubb4b* and *krt8-mNG2$_{11}$* — with each of our mNG2$_{1-10}$ transgenic lines — *fezf2:mNG2$_{1-10}$*, *myl7:mNG2$_{1-10}$*, and *ubb:mNG2$_{1-10}$*. For *mNG2$_{11}$-tubb4b*, crossing to *ubb:mNG2$_{1-10}$* produced fluorescence broadly throughout the head (Fig. 4B–B′), enabling timelapse analysis of tubulin dynamics in the otic vesicle and surrounding region (Video 1). This fluorescence pattern is similar to mNG2$_{1-10}$ mRNA injection and to the reported expression pattern for *tubb4b* (Thisse and Thisse, 2008; Zhuo et al., 2012). In contrast, crossing to *fezf2:mNG2$_{1-10}$* resulted in fluorescence restricted to the brain and eye (Fig. 4C–C′), consistent with the known expression pattern for *fezf2* (Jeong et al., 2006). Finally, crossing to *myl7:mNG2$_{1-10}$* resulted in no observable fluorescence (Fig. 4D). This result is consistent with the

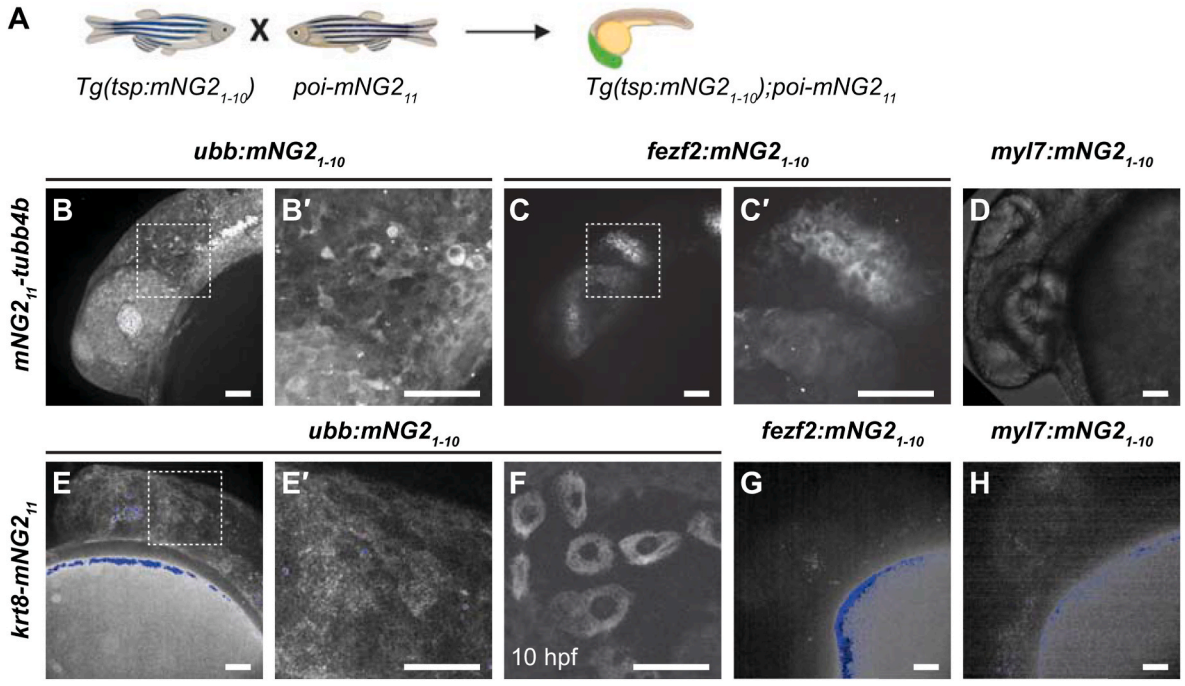

Fig. 4. Combinatorial expression of tissue-specific mNG2$_{1-10}$ and mNG2$_{11}$-tagged proteins. A. Schematic of crossing strategy. tsp, tissue-specific promoter. poi, protein of interest. **B-D.** Representative images of embryos obtained from crossing *mNG2$_{11}$-tubb4b* and *ubb:mNG2$_{1-10}$* (B–B′), *fez2f:mNG2$_{1-10}$* (C–C′), or *myl7:mNG2$_{1-10}$* (D). B′ and C′ show boxed regions in B and C, respectively. **E-H.** Representative images of embryos obtained by crossing *krt8-mNG2$_{11}$* to *ubb:mNG2$_{1-10}$* (E–F), *fez2f:mNG2$_{1-10}$* (G), or *myl7:mNG2$_{1-10}$* (H). E′ shows boxed region in E. Maximum projections of confocal z-stacks. Images were acquired at 24 h post-fertilization (hpf) unless otherwise noted. Image in D has been overexposed to emphasize lack of fluorescence. Autofluorescent speckles (yolk, pigment cells, and debris) are colored blue for display purposes. Scale bars, 50 μm.

reported expression pattern for *tubb4b*, which has not been reported to be expressed in the heart.

The results we obtained for *krt8-mNG2$_{11}$* similarly demonstrated retention of endogenous expression patterns. Crossing to *ubb:mNG2$_{1-10}$* resulted in fluorescence primarily in the skin at 24 hpf (Fig. 4E–E′), similar to mNG2$_{1-10}$ mRNA injection. We also observed fluorescence in cells of the enveloping layer at 10 hpf (Fig. 4F), consistent with the reported expression pattern for *krt8* (Fischer et al., 2014; Thisse and Thisse, 2008). Crossing *krt8-mNG2$_{11}$* to *fezf2:mNG2$_{1-10}$* or *myl7:mNG2$_{1-10}$* resulted in no observable fluorescence (Fig. 4G and H), which is expected as *krt8* has not been reported to be expressed in either cardiac or neural tissues.

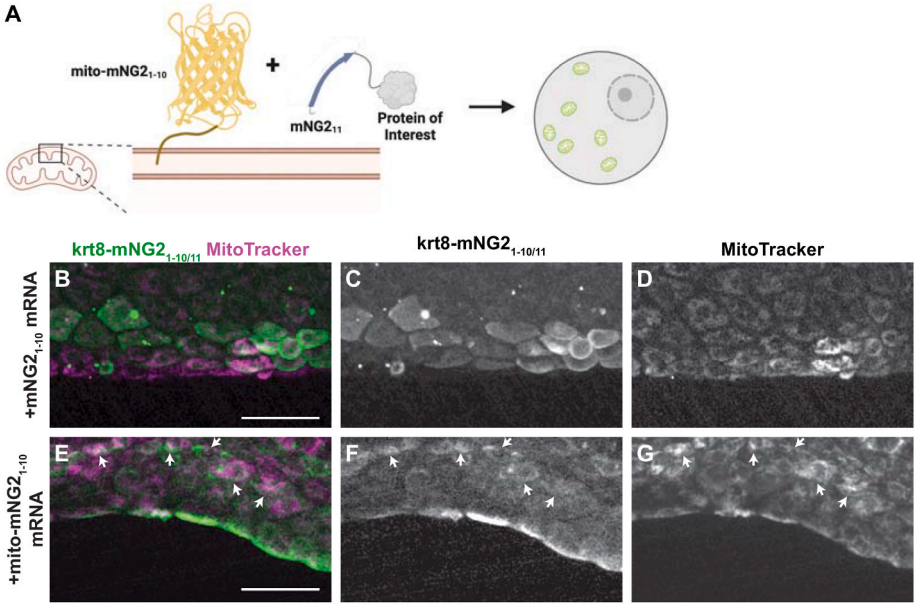

Fig. 5. Directing protein localization with split-mNG2. A. Schematic illustrating use of the split-mNG2 system to sequester proteins of interest on mitochondria. **B–G.** Representative images of *krt8-mNG2$_{11}$* embryos injected with mNG2$_{1-10}$ (B–D) or mito-mNG2$_{1-10}$ (E–G) mRNA and stained with MitoTracker dye to label mitochondria. Maximum projections of confocal z-stacks. Arrows indicate colocalization between split-mNG2 and MitoTracker fluorescence. Images were acquired from the tail fin epidermis at 48 h post-fertilization (hpf). Scale bars, 50 μm.

Altogether, our results show that combining transgenic $mNG2_{1-10}$ expression and $mNG2_{11}$ tagging can achieve tissue-specific fluorescent protein labeling that preserves endogenous expression patterns.

2.5. Directing protein localization with split-mNG2

Given that split-mNG2 fragments self-assemble, it may be possible to use $mNG2_{1-10}$ as a "bait" to direct $mNG2_{11}$-tagged proteins to specific subcellular locations. To determine the feasibility of this application, we fused $mNG2_{1-10}$ to a localization signal for the outer mitochondrial membrane (mito-$mNG2_{1-10}$) (Bear et al., 2000) (Fig. 5A). We then injected mRNA for mito-$mNG2_{1-10}$ into *krt8-mNG2$_{11}$* embryos. Compared to control embryos injected with untagged $mNG2_{1-10}$ (Fig. 5B–D), embryos injected with mito-$mNG2_{1-10}$ exhibited qualitatively different fluorescence localization patterns that co-localized with the mitochondrial dye MitoTracker (Fig. 5E–G). These results suggest that mito-$mNG2_{1-10}$ is indeed directing $mNG2_{11}$-tagged Keratin 8 to the mitochondria. Thus, by anchoring $mNG2_{1-10}$ to specific cellular compartments, the split-mNG2 system can be used to manipulate protein localization.

3. Discussion

In this study, we describe using the $mNG2_{1-10/11}$ split fluorescent protein system to achieve tissue-specific fluorescent labeling of endogenous proteins in zebrafish embryos. We further demonstrate that the split-mNG2 system can be used to control protein localization by anchoring the mNG21-10 fragment to specific cellular compartments.

Similar $FP_{1-10/11}$ systems are now commonly used as endogenous protein labeling tools in cell lines (Cho et al., 2022; Feng et al., 2017; Kamiyama et al., 2016; Leonetti et al., 2016). The popularity of these systems is primarily due to the ease with which the short FP_{11} sequences can be inserted into gene loci. The general utility of split-FP systems for protein labeling has also been demonstrated in multicellular organisms including zebrafish (Kesavan et al., 2021) and mouse embryos (O'Hagan et al., 2021), but in these studies the corresponding FP_{1-10} fragment was delivered constitutively. Tissue specificity has been achieved in *C. elegans* (Goudeau et al., 2021; He et al., 2019; Hefel and Smolikove, 2019; Noma et al., 2017) and *Drosophila* (Kamiyama et al., 2021) and now in zebrafish (this study). The ability to spatially restrict fluorescent labeling is especially advantageous for studying the tissue-specific function of an otherwise broadly expressed protein. In such cases, constitutive protein labeling would obscure the area under study due to competing signals coming from surrounding tissues, which cannot be easily removed without advanced microscopy or image processing methods. In contrast, our split-mNG2-based approach can achieve tissue-specific labeling using relatively straightforward and conventional techniques.

In this study, we demonstrated a novel application of the split-mNG2 system to control of protein localization via tethering Keratin 8 to mitochondria (Fig. 5). There are several potential applications for using the split-mNG2 system to experimentally manipulate protein localization. For example, $mNG2_{11}$-tagged proteins could be sequestered away from their normal site of function to achieve a loss-of-function effect. The same approach could also be used to achieve gain-of-function effects by constitutively anchoring a protein to its site of action or to an ectopic location. This approach could also be used to manipulate the properties of specific organelles or subcellular compartments through recruitment of $mNG2_{11}$-tagged enzymes. An advantage of the split-mNG2 approach is that successful (mis)localization can easily be confirmed because the reconstituted mNG21-10/11 complexes retain their fluorescence. When combined with transgenic expression of $mNG2_{1-10}$, this approach can be applied to specific tissues of interest for even broadly expressed proteins.

Previous reports have suggested that not all proteins can be easily labeled with the split-mNG2 system (Cho et al., 2022; Leonetti et al., 2016; O'Hagan et al., 2021). Fluorescent labeling may fail because the target protein does not tolerate $mNG2_{11}$ tagging. Thus, $mNG2_{11}$ fusion proteins should be designed using the same considerations as with any epitope tag. Fluorescence brightness might also be a challenge. Split-FP systems are known to be dimmer than their intact counterparts; for example, split-mNG2 is about 60% as bright as intact mNeonGreen (Feng et al., 2017). Thus, even if tagging is tolerated, some proteins may not be expressed at high enough levels to produce a detectable fluorescent signal (Leonetti et al., 2016; O'Hagan et al., 2021). This challenge could be overcome by inserting multiple repeats of the $mNG2_{11}$ sequence to increase fluorescent signal as has been demonstrated for split-GFP (He et al., 2019; Hefel and Smolikove, 2019; Kamiyama et al., 2016, 2021; Noma et al., 2017). Additionally, a third generation split-mNG system was recently developed and reported to have improved spectral properties (Zhou et al., 2020), which may extend the use of split-FP labeling to low or moderately expressed proteins. A challenge specific to working with multicellular organisms is the difficulty of detecting fluorescence in very thick samples, such as late larval and older zebrafish stages. However, our demonstration that split-mNG2 fluorescence is preserved after paraformaldehyde fixation (Fig. S1) suggests that our method is compatible with tissue sectioning protocols.

In this study, we focused on the use of split-mNG2 as a protein labeling tool. However, the ability to control expression of these protein fragments independently, paired with their ability to self-assemble, could be leveraged for other applications. For example, they could be used as coincidence detectors to monitor cell states or signaling pathway activation. And because fluorescence is only produced when the two fragments bind, they could be used to visualize interactions at multiple length scales, i.e., between proteins, organelles, cells, or adjacent tissues.

4. Conclusions

In summary, we have demonstrated that the split-mNG2 system can function in zebrafish to endogenously label proteins in a tissue-specific manner, with other potential applications that make it broadly useful to many areas of investigation.

5. Materials and methods

5.1. Zebrafish strains

Adult *Danio rerio* zebrafish were maintained under standard laboratory conditions. Zebrafish in an outbred *AB*, *TL*, or *EKW* background were used as wild-type strains. Strains generated in this study are: *Tg(fezf2:mNG2$_{1-10}$)^{ucm120}*; *Tg(myl7:mNG2$_{1-10}$)^{ucm121}*; *Tg(ubb:mNG2$_{1-10}$)^{ucm117}*; *krt8^{ucm132}*; and *tubb4b^{ucm132}*. This study was performed with the approval of the Institutional Animal Care and Use Committee (IACUC) of the University of California Merced (Protocol #2023-1144).

5.2. mRNA expression

All expression plasmids for *in vitro* mRNA synthesis were generated in a pCS2 backbone. To generate pCS2-GFP_{1-10}, GFP_{1-10} was PCR amplified from pACUH- GFP_{1-10} (Bo Huang, University of California San Francisco) and cloned into pCS2 by enzymatic assembly (Gibson et al., 2009). To generate pCS2-$mNG2_{1-10}$, $mNG2_{1-10}$ was PCR amplified from pSFFV- $mNG2_{1-10}$ (Bo Huang, University of California San Francisco) and cloned into pCS2 by enzymatic assembly. To generate pCS2-GFP_{11}-H2B and pCS2-$mNG2_{11}$-H2B, GFP_{11} (5'-CGTGACCA-CATGGTCCTTCATGAGTATGTAAATGCTGCTGGGATTACA-3') and $mNG2_{11}$ (5'-ACCGAGCTCAACTTCAAGGAGTGGCAAAAGGCCTTTACC-GATATGATG-3') were directly synthesized by Integrated DNA Technologies and H2B was PCR amplified from GFP-H2B (Hesselson et al., 2009); fragments were fused and cloned into pCS2 by enzymatic assembly. To generate pCS2-mito-$mNG2_{1-10}$, the outer mitochondrial membrane signal sequence was PCR amplified from pMSCV-FPPPP-mito

(Bear et al., 2000) and cloned into pCS2-mNG2$_{1-10}$ by enzymatic assembly. Capped messenger RNA was synthesized using the mMESSAGE mMACHINE kit (Ambion), and 500 pg of each mRNA was injected at the one- or two-cell stage.

5.3. Generation of *mNG2$_{1-10}$* transgenic lines

All transgene plasmids were generated in a pμTol2 backbone (LaBelle et al., 2021). mNG2$_{1-10}$ and promoter sequences for *fezf2* (Berberoglu et al., 2009), *myl7* (Huang et al., 2003), or *ubb* (Mosimann et al., 2011) were PCR amplified then fused and cloned into pμTol2 by enzymatic assembly to generate pμTol2-fez:mNG2$_{1-10}$, pμTol2-myl7:mNG2$_{1-10}$, and pμTol2-ubb:mNG2$_{1-10}$, respectively. The constructs were used to generate *Tg(fez:mNG2$_{1-10}$)^{ucm120}*; *Tg(myl7:mNG2$_{1-10}$)^{ucm121}*; *Tg(ubb:mNG2$_{1-10}$)^{ucm117}* using standard transgenesis protocols (Clark et al., 2011; Kawakami, 2004).

5.4. CRISPR/Cas-directed insertion of *mNG2$_{11}$*

Guide RNAs (gRNAs) were designed using CRISPRscan (Moreno-Mateos et al., 2015) and synthesized as previously described (Varshney et al., 2016). The double-stranded DNA template for homology directed repair was assembled from two oligomers synthesized by Integrated DNA Technologies. Each oligomer contained the sequence for mNG2$_{11}$, a 10-amino acids-encoding linker sequence (5′-GGAGCTGGTGCAGGCGCTGGAGCCGGTGCC-3′), and a homology arm. Oligomers were hybridized to obtain a double-stranded template with single-stranded, 30 bp-long homology arms at each end (Liang et al., 2017). gRNAs, donor DNA, and Cas9 mRNA were injected at the one-cell stage as previously described (Gagnon et al., 2014).

To verify insertion, we pooled 40 injected embryos at 24 hpf, isolated genomic DNA, and performed PCR using two sets of primer pairs per gene covering the 5′ and 3′ insertion sites. The same primer sets were used for quantitative PCR (qPCR) to estimate knock-in efficiency. Each qPCR reaction contained 2X PerfeCTa® SYBR Green FastMix (Quantabio), five-fold diluted genomic DNA, and 325 nM of each primer. Reactions were carried out on a QuantStudio3 (Applied Biosystems) real-time PCR machine using the following program: initial activation at 95 °C for 10 min, followed by 40 cycles of 30 s at 95 °C, 30 s at 60 °C, and 1 min at 72 °C. Once the PCR was completed, a melt curve analysis was performed to determine reaction specificity. The gene *prox1a* was used as a reference. Primers used in this study (presented 5′–3′):

5′ h2az2b-mNG211 forward: TTGTGTGTTTGTGCGTCCGC.
5′ h2az2b-mNG211 reverse: GCCACTCCTTGAAGTTGAGC.
3′ h2az2b-mNG211 forward: GCTCAACTTCAAGGAGTGGC.
3′ h2az2b-mNG211 reverse: ACGAAGCCCCGAAAGCACAC.
5′ mNG211-krt8 forward: ATACAGCGGCGGATACAGCG.
5′ mNG211-krt8 reverse: GCCACTCCTTGAAGTTGAGC.
3′ mNG211-krt8 forward: GCTCAACTTCAAGGAGTGGC.
3′ mNG211-krt8 reverse: AAGGCACGACAAGAGCGGTG.
5′ mNG211-tubb4b forward: CACATCTCGAATTACGACCTCA.
5′ mNG211-tubb4b reverse: GCCTTTTGCCACTCCTTGAAG.
3′ mNG211-tubb4b forward: GCTCAACTTCAAGGAGTGGC.
3′ mNG211-tubb4b reverse: AAAACAAGCAAGGATTAGCGTC
prox1a forward: TGTCATTTGCGCTCGCGCTG prox1a
reverse: ACCGCAACCCGAAGACAGTG.

To verify germline transmission and establish stable lines, injected F$_0$ embryos were raised to adulthood then outcrossed to wild-type zebrafish. We pooled 40 of the resulting F$_1$ embryos at 24 hpf, isolated genomic DNA, and performed PCR using the same primer sets as above. PCR fragments were cloned into pGEM-T (Promega), and the inserts were sequenced by Sanger sequencing (University of California Berkeley DNA Sequencing Facility). Only clutches containing precise insertion of the mNG2$_{11}$ plus linker sequence were kept for propagation. At adulthood, individual F$_1$ zebrafish were genotyped by fin clipping using the same primer sets as described above. Only animals containing precise insertion of the mNG2$_{11}$ sequence were kept for line propagation.

5.5. Microscopy and image processing

Dechorionated embryos or larvae were embedded in 1.5% low-melting agarose (ISC BioExpress) containing 0.01% tricaine (Sigma-Aldrich) within glass-bottom Petri dishes (MatTek Corporation). For mitochondria labeling, embryos were incubated in 50 nM MitoTracker Red CMXRos (Invitrogen) for 30 min prior to agarose embedding. For paraformaldehyde fixation, embryos were incubated in 4% paraformaldehyde (Sigma-Aldrich) overnight at 4 °C, washed three times for 10 min in 1X phosphate buffered saline with 0.1% Tween-20 (Sigma-Aldrich) at room temperature, then embedded in agarose for imaging. Identical image acquisition settings were used for all embryos from the same set of experiments.

Widefield fluorescence and brightfield images were acquired on an Olympus SZX16 stereomicroscope equipped with a DP23 monochrome camera and cellSens software (Evident). Brightfield images were acquired with transmitted light from an LED diascopic base (Evident). GFP or mNG2 fluorescence was excited with an LED light source (X-Cite) and 470/40 nm excitation filter (Chroma) and acquired with a 500 nm long-pass emission filter (Chroma).

Confocal images were acquired on an Olympus IX83 microscope (Evident) equipped with a spinning disk confocal unit (CSU–W1; Andor). Brightfield images were acquired using a transmitted LED light source. GFP or mNG2 fluorescence was excited with a 488 nm 150 mW solid state laser (Visitron Systems) and collected with a 525/50 nm emission filter. Images were acquired with a Prime 95b sCMOS camera (Teledyne Photometrics) controlled with MicroManager software (Edelstein et al., 2014). Z-stack optical sections were collected with a 10x/0.4NA objective lens (Evident) with a step-size of 5 μm or with a 30x/1.05 NA objective lens (Evident) with a step-size of 2 μm using a Piezo focus motor (ASI). For time-lapse experiments, z-stacks with a step-size of 4 μm were collected with a 30x/1.05 NA objective lens every 5 min, using an exposure time of 200 ms and 1 × 1 camera binning. All z-stacks are displayed as maximum z-projections.

Images were processed identically for each set of experiments using Fiji software (Schindelin et al., 2012) as follows: denoised using the Non-local Means Denoise plugin (Buades et al., 2005), brightness and contrast levels adjusted, converted to 8-bit depth, and cropped. In cases where the region of interest extended beyond the microscope's field of view, multiple images were stitched together using the pairwise stitching plugin. Brightfield and fluorescence images were merged in Photoshop software (Adobe). Illustrations were created with BioRender (https://biorender.com).

CRediT authorship contribution statement

Gloria D. Ligunas: Writing – review & editing, Writing – original draft, Visualization, Project administration, Investigation, Formal analysis, Data curation. **German F. Paniagua:** Writing – review & editing, Writing – original draft, Visualization, Project administration, Investigation, Formal analysis, Data curation. **Jesselynn LaBelle:** Writing – review & editing, Investigation. **Adela Ramos-Martinez:** Writing – review & editing, Investigation. **Kyle Shen:** Writing – review & editing, Investigation. **Emma H. Gerlt:** Writing – review & editing, Investigation. **Kaddy Aguilar:** Writing – review & editing, Investigation. **Ngoc Nguyen:** Writing – review & editing, Investigation. **Stefan C. Materna:** Writing – review & editing, Visualization, Supervision, Project administration, Methodology, Investigation, Funding acquisition, Formal analysis. **Stephanie Woo:** Writing – review & editing, Writing – original draft, Visualization, Supervision, Project administration, Investigation, Funding acquisition, Data curation, Conceptualization.

Data availability

Data will be made available on request.

Acknowledgements

We thank Bo Huang (University of California San Francisco) for providing the split-GFP and split-mNG2 plasmids and advice, Anne Pipathsouk (University of California San Francisco) and Manuel Leonetti (Chan Zuckerberg Biohub) for helpful discussions, the Department of Animal Research Services (University of California Merced) for excellent fish care, and members of the Woo and Materna labs for helpful comments on the manuscript. This work was supported by grants from the Society for Developmental Biology, the National Institutes of Health (NIH R15HD102829), and the National Science Foundation (NSF-IOS-2238304) to S.W. J.L. was supported by a National Institutes of Health training grant (NIH T32GM141862). K.S. received support from the National Science Foundation (NSF-CREST: Center for Cellular and Biomolecular Machines at the University of California, Merced, NSF-HRD-1547848).

Appendix A. Supplementary data

Supplementary data to this article can be found online at https://doi.org/10.1016/j.ydbio.2024.06.011.

References

Albadri, S., Del Bene, F., Revenu, C., 2017. Genome editing using CRISPR/Cas9-based knock-in approaches in zebrafish. Methods San Diego Calif 121–122, 77–85.

Auer, T.O., Del Bene, F., 2014. CRISPR/Cas9 and TALEN-mediated knock-in approaches in zebrafish. Methods San Diego Calif 69, 142–150.

Bear, J.E., Loureiro, J.J., Libova, I., Fässler, R., Wehland, J., Gertler, F.B., 2000. Negative regulation of fibroblast motility by Ena/VASP proteins. Cell 101, 717–728. https://doi.org/10.1016/s0092-8674(00)80884-3.

Berberoglu, M.A., Dong, Z., Mueller, T., Guo, S., 2009. fezf2 expression delineates cells with proliferative potential and expressing markers of neural stem cells in the adult zebrafish brain. Gene Expr. Patterns 9, 411–422. https://doi.org/10.1016/j.gep.2009.06.002.

Buades, A., Coll, B., Morel, J.-M., 2005. A non-local algorithm for image denoising. In: 2005 IEEE Comput. Soc. Conf. Comput. Vis. Pattern Recognit. CVPR05, vol. 2. IEEE, San Diego, CA, USA, pp. 60–65. https://doi.org/10.1109/CVPR.2005.38.

Cho, N.H., Cheveralls, K.C., Brunner, A.-D., Kim, K., Michaelis, A.C., Raghavan, P., et al., 2022. OpenCell: endogenous tagging for the cartography of human cellular organization. Science 375, eabi6983. https://doi.org/10.1126/science.abi6983.

Clark, K.J., Urban, M.D., Skuster, K.J., Ekker, S.C., 2011. Transgenic zebrafish using transposable elements. Methods Cell Biol. 104, 137–149.

Edelstein, A.D., Tsuchida, M.A., Amodaj, N., Pinkard, H., Vale, R.D., Stuurman, N., 2014. Advanced methods of microscope control using μManager software. J Biol Methods 1, e10. https://doi.org/10.14440/jbm.2014.36.

Feinberg, E.H., Vanhoven, M.K., Bendesky, A., Wang, G., Fetter, R.D., Shen, K., et al., 2008. GFP Reconstitution across Synaptic Partners (GRASP) defines cell contacts and synapses in living nervous systems. Neuron 57, 353–363.

Feng, S., Sekine, S., Pessino, V., Li, H., Leonetti, M.D., Huang, B., 2017. Improved Split Fluorescent Proteins for Endogenous Protein Labeling, vol. 8, p. 370.

Fischer, B., Metzger, M., Richardson, R., Knyphausen, P., Ramezani, T., Franzen, R., et al., 2014. p53 and TAp63 promote keratinocyte proliferation and differentiation in breeding tubercles of the zebrafish. PLoS Genet. 10, e1004048 https://doi.org/10.1371/journal.pgen.1004048.

Gagnon, J.A., Valen, E., Thyme, S.B., Huang, P., Akhmetova, L., Pauli, A., et al., 2014. Efficient mutagenesis by Cas9 protein-mediated oligonucleotide insertion and large-scale assessment of single-guide RNAs. PLoS One 9, e98186. https://doi.org/10.1371/journal.pone.0098186.

Gibson, D.G., Young, L., Chuang, R.-Y., Venter, J.C., Hutchison, C.A., Smith, H.O., 2009. Enzymatic assembly of DNA molecules up to several hundred kilobases. Nat. Methods 6, 343–345.

Goudeau, J., Sharp, C.S., Paw, J., Savy, L., Leonetti, M.D., York, A.G., et al., 2021. Split-wrmScarlet and split-sfGFP: tools for faster, easier fluorescent labeling of endogenous proteins in Caenorhabditis elegans. Genetics 217, iyab014. https://doi.org/10.1093/genetics/iyab014.

Harvey, S.A., Smith, J.C., 2009. Visualisation and quantification of morphogen gradient formation in the zebrafish. PLoS Biol. 7, e1000101.

He, S., Cuentas-Condori, A., Miller, D.M., 2019. NATF (native and tissue-specific fluorescence): a strategy for bright, tissue-specific GFP labeling of native proteins in Caenorhabditis elegans. Genetics 212, 387–395. https://doi.org/10.1534/genetics.119.302063.

Hefel, A., Smolikove, S., 2019. Tissue-specific split sfGFP system for streamlined expression of GFP tagged proteins in the Caenorhabditis elegans germline. G3 Bethesda Md 9, 1933–1943. https://doi.org/10.1534/g3.119.400162.

Hesselson, D., Anderson, R.M., Beinat, M., Stainier, D.Y.R., 2009. Distinct populations of quiescent and proliferative pancreatic beta-cells identified by HOTcre mediated labeling. Proc. Natl. Acad. Sci. U. S. A. 106, 14896–14901. https://doi.org/10.1073/pnas.0906348106.

Huang, C.-J., Tu, C.-T., Hsiao, C.-D., Hsieh, F.-J., Tsai, H.-J., 2003. Germ-line transmission of a myocardium-specific GFP transgene reveals critical regulatory elements in the cardiac myosin light chain 2 promoter of zebrafish. Dev Dyn. Off Publ. Am. Assoc. Anat . 228, 30–40.

Jeong, J.-Y., Einhorn, Z., Mercurio, S., Lee, S., Lau, B., Mione, M., et al., 2006. Neurogenin1 is a determinant of zebrafish basal forebrain dopaminergic neurons and is regulated by the conserved zinc finger protein Tof/Fezl. Proc. Natl. Acad. Sci. U. S. A. 103, 5143–5148. https://doi.org/10.1073/pnas.0600337103.

Kamiyama, D., Sekine, S., Barsi-Rhyne, B., Hu, J., Chen, B., Gilbert, L.A., et al., 2016. Versatile protein tagging in cells with split fluorescent protein. Nat. Commun. 7, 11046.

Kamiyama, R., Banzai, K., Liu, P., Marar, A., Tamura, R., Jiang, F., et al., 2021. Cell-type-specific, multicolor labeling of endogenous proteins with split fluorescent protein tags in Drosophila. Proc. Natl. Acad. Sci. U. S. A. 118, e2024690118 https://doi.org/10.1073/pnas.2024690118.

Kawakami, K., 2004. Transgenesis and gene trap methods in zebrafish by using the Tol2 transposable element. Methods Cell Biol. 77, 201–222.

Kesavan, G., Machate, A., Brand, M., 2021. CRISPR/Cas9-Based split fluorescent protein tagging. Zebrafish 18, 369–373. https://doi.org/10.1089/zeb.2021.0031.

Kimura, Y., Hisano, Y., Kawahara, A., Higashijima, S.-I., 2014. Efficient generation of knock-in transgenic zebrafish carrying reporter/driver genes by CRISPR/Cas9-mediated genome engineering. Sci. Rep. 4, 6545.

LaBelle, J., Ramos-Martinez, A., Shen, K., Motta-Mena, L.B., Gardner, K.H., Materna, S. C., et al., 2021. Tael 2.0: an improved optogenetic expression system for zebrafish. Zebrafish 18, 20–28.

Leonetti, M.D., Sekine, S., Kamiyama, D., Weissman, J.S., Huang, B., 2016. A scalable strategy for high-throughput GFP tagging of endogenous human proteins. Proc. Natl. Acad. Sci. U. S. A. 113, E3501–E3508.

Liang, X., Potter, J., Kumar, S., Ravinder, N., Chesnut, J.D., 2017. Enhanced CRISPR/Cas9-mediated precise genome editing by improved design and delivery of gRNA, Cas9 nuclease, and donor DNA. J. Biotechnol. 241, 136–146.

Moreno-Mateos, M.A., Vejnar, C.E., Beaudoin, J.-D., Fernandez, J.P., Mis, E.K., Khokha, M.K., et al., 2015. CRISPRscan: designing highly efficient sgRNAs for CRISPR-Cas9 targeting in vivo. Nat. Methods 12, 982–988.

Mosimann, C., Kaufman, C.K., Li, P., Pugach, E.K., Tamplin, O.J., Zon, L.I., 2011. Ubiquitous transgene expression and Cre-based recombination driven by the ubiquitin promoter in zebrafish. Dev. Camb. Engl. 138, 169–177.

Noma, K., Goncharov, A., Ellisman, M.H., Jin, Y., 2017. Microtubule-dependent ribosome localization in C. elegans neurons. Elife 6, e26376. https://doi.org/10.7554/eLife.26376.

O'Hagan, D., Kruger, R.E., Gu, B., Ralston, A., 2021. Efficient generation of endogenous protein reporters for mouse development. Dev. Camb. Engl. 148, dev197418 https://doi.org/10.1242/dev.197418.

Rosen, J.N., Sweeney, M.F., Mably, J.D., 2009. Microinjection of zebrafish embryos to analyze gene function. J. Vis. Exp. 1115 https://doi.org/10.3791/1115.

Schindelin, J., Arganda-Carreras, I., Frise, E., Kaynig, V., Longair, M., Pietzsch, T., et al., 2012. Fiji: an open-source platform for biological-image analysis. Nat. Methods 9, 676–682. https://doi.org/10.1038/nmeth.2019.

Simiczyjew, A., Mazur, A.J., Popow-Woźniak, A., Malicka-B\laszkiewicz, M., Nowak, D., 2014. Effect of overexpression of β- and γ-actin isoforms on actin cytoskeleton organization and migration of human colon cancer cells. Histochem. Cell Biol. 142, 307–322.

Thisse, C., Thisse, B., 2008. High-resolution in situ hybridization to whole-mount zebrafish embryos. Nat. Protoc. 3, 59–69.

Varshney, G.K., Carrington, B., Pei, W., Bishop, K., Chen, Z., Fan, C., et al., 2016. A high-throughput functional genomics workflow based on CRISPR/Cas9-mediated targeted mutagenesis in zebrafish. Nat. Protoc. 11, 2357–2375. https://doi.org/10.1038/nprot.2016.141.

Zhang, Y., Marshall-Phelps, K., De Almeida, R.G., 2023. Fast, precise and cloning-free knock-in of reporter sequences *in vivo* with high efficiency. Development 150, dev201323. https://doi.org/10.1242/dev.201323.

Zhou, S., Feng, S., Brown, D., Huang, B., 2020. Improved yellow-green split fluorescent proteins for protein labeling and signal amplification. PLoS One 15, e0242592. https://doi.org/10.1371/journal.pone.0242592.

Zhuo, H.-Q., Huang, L., Huang, H.-Q., Cai, Z., 2012. Effects of chronic tramadol exposure on the zebrafish brain: a proteomic study. J. Proteonomics 75, 3351–3364. https://doi.org/10.1016/j.jprot.2012.03.038.